2007 IEEE International Conference on
Robotics and Automation
Roma, Italy, 10-14 April 2007

Passive Foot Design and Contact Area Analysis for Climbing Mini-Whegs™

Kathryn A. Daltorio, Terence E. Wei, Stanislav N. Gorb, Roy E. Ritzmann, Roger D. Quinn

***Abstract*—Mini-Whegs™, a power-autonomous vehicle that uses multi-spoke wheel-legs for locomotion, is able to climb vertical glass surfaces with several different wheel-leg designs. Adhesion to the glass is achieved using pressure sensitive adhesives. In this paper, high-speed video is used to compare the performance and contact area during steps of five passive foot designs. The contact area, when normalized by the leg length, may help explain the differences in performance between several designs.**

I. Introduction

CLIMBING steep substrates expands the functional workspace of a climbing robot. A robot that would otherwise be confined to the ground could inspect difficult-to-access ceilings, clean high windows, or explore deep shafts. For space applications, novel attachment mechanisms may be required to anchor a robot to a work surface in the absence of gravity and air pressure.

Using passive suction cups on glass [1][2] or electromagnets on metal [3], robots can be specialized to climb a specific substrate. Robots for climbing more complex surfaces such as ordinary walls [4][5], rock-climbing walls [6] or trees [7] may make use of active attachment mechanisms, more degrees of freedom or more advanced control systems. Each vehicle must be carefully designed because additional complexity tends to increase the weight of an autonomous robot, which requires that the feet provide more adhesion to maintain reliable attachment. Investigating passive attachment mechanisms may lead to lighter autonomous climbing robots.

In nature, many small animals such as insects and lizards rely on climbing. The active claws, passive spines, and smooth adhesive pads of cockroaches allow them to climb rough and smooth substrates [8]. Like an insect, SpinybotII can ascend rough vertical surfaces using compliant arrays of spines [9]. For smooth surfaces, beetles and Tokay geckos adhere to surfaces using patches of microscopic hairs that provide a mechanism for dry adhesion [10]. Inspired by these animal mechanisms, new adhesives are being developed [11][12]. A few climbing robot designs, such as Waalbots [13] and MechoGecko [14], have been tested with traditional adhesives.

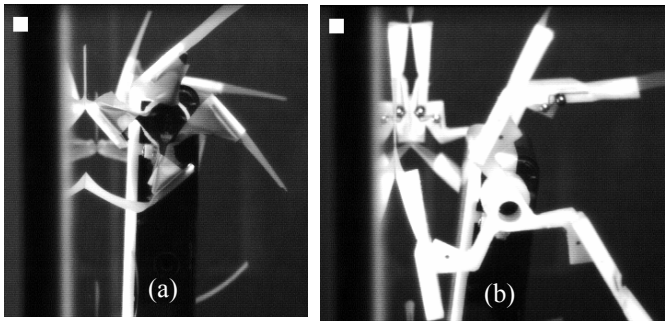

Fig. 1. Mini-Whegs™ with (a) four-spoke black Delrin® wheel-legs and (b) three-spoke white Delrin® wheel-legs with ankle joints.

As these climbing robots have shown, the kinematics of the end-effecters are as critical as the tenacity of the adhesive material. Single gecko setae require very specific motions to attach and release [10]. Geckos and some insects [15] apply the entire attachment organ on contact, but detach gradually.

Previously, we demonstrated that a simple, passive, adhesive foot can be designed that converts the ground walking Mini-Whegs™ [16] into a wall and ceiling climbing robot , which can be used to test new bio-inspired adhesive technologies. Whegs™, like PROLERO [17] and RHex [18] have legs driven in an arc like the spokes of a wheel [19]. The foot kinematics of the resulting robot, Climbing Mini-Whegs™ [20], appear similar to the quick attachment and peeling detachment of some insects and geckos.

Shown in Fig. 2, the radio-controlled robot (5.4 cm by 8.9 cm, 87 grams) is power-autonomous and has a total of four wheel-legs, each with three or four spokes The feet are attached to the ends of the spokes and the flexibility of the feet acts as a hinge between the feet and spokes. The feet

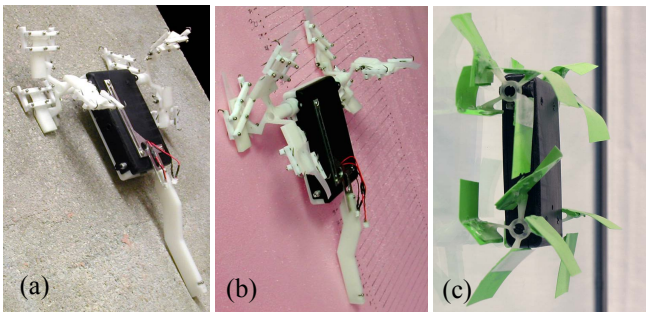

Fig. 2. Mini-Whegs ™ climbing with white wheel-legs on (a) porous concrete and (b) soft Styrofoam. Mini-Whegs can also climb glass with biologically inspired structured material (c).

Manuscript received September 15, 2006. This work was supported by the Intelligence Community (IC) Postdoctoral Fellowship Program under National Geospatial Intelligence Agency contract HM1582-05-1-2021, and by the National Science Foundation under NSF/IGERT grant DGE-9972747.

K. A. Daltorio, T. E. Wei, and R. D. Quinn are with the Mechanical Engineering Department of Case Western Reserve University, Cleveland, OH 44106, USA; phone: 216-368-5216; (e-mails: kathryn.daltorio@case.edu, t@fluggart.com, roger.quinn@case.edu) http://biorobots.case.edu

S. N. Gorb is with the Evolutionary Biomaterials Group at Max-Planck-Institute for Metals Research, 70569 Stuttgart, Germany; (email: S.Gorb@mf.mpg.de)

R. E. Ritzmann is with the Department of Biology at Case Western Reserve University, Cleveland, OH 44106, USA; (e-mail: roy.ritzmann@case.edu).

contact the substrate, bend as the hub turns, peel off the substrate gradually, and spring back to their initial position for the next contact. It was previously reported that this robot could climb glass walls and ceilings using standard pressure-sensitive adhesives [20] as well as reusable, biologically-inspired adhesives [21]. This vehicle has also been fitted with wheel-legs with compliant ankles that can be fitted with sharp spines for climbing on rough and soft substrates [22].

While several climbing robot designs utilizing adhesives have been described [13][14][20], this is the first time an analysis of the foot contact area created by a climbing robot has been reported. High-speed video was used to investigate and compare the performance and mechanics of the two different sets of wheel-legs, using standard, pressure-sensitive adhesive at five different cross-sectional profiles, (see Table I). The methods used in this paper also apply to dry adhesives, such as the structured material previously used on this robot [21].

II. Description of Spoked Appendages Tested

Two different types of appendages were tested on the robot. The first were four-spoke, black one-piece wheel-legs (see Fig. 3a). The second were three-spoke white wheel-legs with separate foot pieces attached with torsion springs (Fig. 3c). Both were fabricated from Delrin®. For convenience, they will be referred to as the white wheel-legs and the black wheel-legs. The black wheel-legs have a smaller circumscribed diameter than the white wheel-legs. Both wheel-leg designs were able to walk on vertical glass surfaces. Note that the term 'foot' will be used here to mean the part of the wheel leg that is nearly parallel to the substrate during application. Therefore, in the black wheel-legs, the 'foot' is the tape and distal flat area on which it is mounted. In the white wheel-legs, the 'foot' is the tape and the plastic foot piece. The legs or spokes are the supports between the feet and the drive axle.

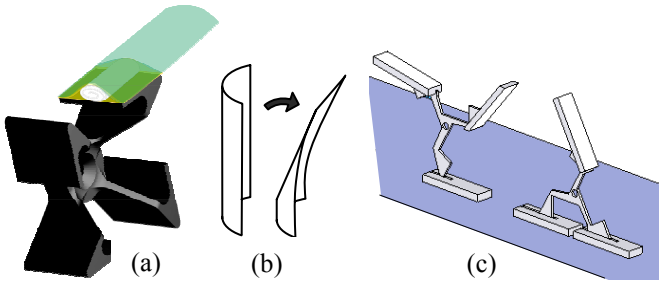

Fig. 3. (a) The sticky side of the tape (shown in green) faces up in this rendering of a black front wheel-leg. Double-sided tape (shown in yellow) holds the tape and the stiffening roll of paper (shown in white) to the wheel-leg. Three other adhesive feet are not shown on wheel-leg. (b) The arced profile of the tape in the A configuration flattens when deformed by the substrate. On the white wheel-legs (c) there are three spokes, each with a foot piece held at the proper orientation by a torsion spring.

TABLE I
Tested Configurations of Wheel- Legs

Name	Wheel-Legs	Leg Length	Center Height[a]	Layers of Tape	Tape Length	Arc Height	Number of Trials[b]
FS	Black, one-piece, 4 spokes	19 mm	15 mm	1	15 mm	0 mm	4
FD		19 mm	15 mm	2	15 mm	0 mm	10+[c]
A		19 mm	15 mm	1	15 mm	2.4 mm	10+[c]
WS	White, jointed ankles, 3 spokes	24 mm[d]	19 mm	1	19 mm	3.5 mm	1-2
WD		24 mm[d]	19 mm	2	19 mm	3.5 mm	6

All testing was done with 0.5 inch (12.7mm) wide Magic Scotch™ tape
[a] The average distance from the geometric center of the robot to the substrate (measured from high-speed video)
[b] The number of 30 cm walks on the glass before performance is unreliable and tape on front feet is replaced.
[c] After 10 runs, stopped gathering data
[d] Distance between hub center and ankle.

The black wheel-legs were tested in three different configurations, with the tape extending flat from the bonding areas (Flat Single or "FS"), with two layers of tape extending (Flat Double or "FD"), and with a roll of paper causing the tape to be arced (Arced or "A") as seen in Fig. 3b. If the tape is considered a cantilevered beam, then using two layers of tape doubles the stiffness in tension and increases the beam stiffness by a factor of eight.

Distinguishing the white wheel-legs from the black ones is that each front leg has a single-degree-of-freedom ankle. The purpose of the ankle was to maintain the orientation of the foot with respect to the substrate. The plastic part of the foot had to provide a long enough lever arm for sharp, penetrating spines (not attached in these tests) to overcome the ankle torque created by the torsion spring when climbing soft substrates. To accommodate the required length, three longer spokes were used. After a foot detaches from the substrate, a torsion spring with stiffness of 8.9×10^{-4} Nm/radian at the ankle joint returns the foot to the proper orientation for the next step [22]. The ankles are located at a radius of 24mm away from the front wheel-leg axles. Rear wheel-legs were similar to black rear wheel-legs.

The white wheel-legs did not attach reliably to the surface when the profile of the tape was flat. Therefore, the surface of each foot piece was cut to have an arced profile. The curved outer surface of the foot pieces served the same purpose as the rolls of paper on the black wheel-legs: the tape attached to them had a curved profile, and thus, was directionally-stiffened (Fig. 3b). These feet were tested with a single layer of tape (White Single or "WS") and with a double layer of tape (White Double or "WD").

III. Methods

A. High-Speed Video Recording

Two synchronized black and white video cameras recorded the robot walking up a vertical glass surface at 250 frames per second. Each frame of video from the cameras had a resolution of 480 pixels by 420 pixels. The "approach" camera, a Redlake model PCI 500, viewed the robot's sagittal plane to record the motion of the adhesive as it attached and detached. The "contact" camera, a Redlake PCI 1000 S model, was directed through the glass at the ventral surface of the robot (see Figure 4). The cameras and lighting were adjusted to maximize the contrast between the

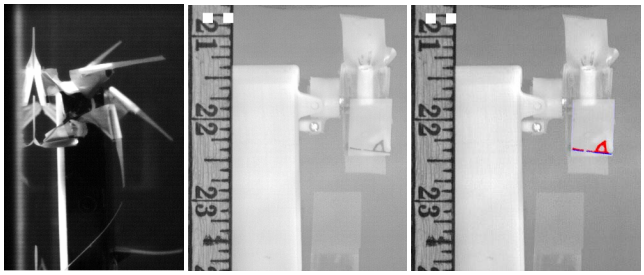

Fig. 4. Images taken at the same instant during A configuration test. The approach camera (a) records the robot from the side as it climbs vertically and the contact camera (b) simultaneously records the robot through the glass substrate. The approach camera data determines step timing and the contact camera measures contact area. One of the resulting contact images with the contacting areas shown in red and the just peeled areas in blue (c). Scale on left in inches.

contacting (darker) and non-contacting (lighter) regions of the adhesive. The lighting conditions were maintained as consistent as possible throughout the testing.

Before each run, the robot was placed on the vertical glass surface several steps below the range of the cameras and commanded to walk at constant speed. Runs in which the robot fell or stalled were not included in this analysis. The tape on the front feet was replaced as needed. The tape on the back feet rarely needed replacement. In fact, for the black wheel-legs, performance of the robot on flat vertical glass was unaffected when the tape on the rear wheel-legs was reversed so that the sticky side never contacted the substrate.

B. Measuring the Contact Area

The darker regions of the adhesive on the glass are in contact with the substrate. Each frame from the recorded video was analyzed to determine the size of the dark region (Fig 4). The user defines the boundaries of the adhesive tape in the image. The algorithm takes three passes through the image sequences. In the first pass, the algorithm identifies likely contact points by determining which have gray values 92% less than the median of the local tile of points 31 pixels wide by 31 pixels high. In the second pass, the median of a 31 by 31 pixel tile is again used, but all the points identified in the first pass as in contact were excluded from the calculation of the median. Again, 92% of the median is the threshold below which gray values are considered in contact. Because simply counting these pixels resulted in graphs that didn't accurately represent the perceived changes in contact area, the area was measured as a fuzzy set. If the threshold minus the gray value of the pixel is negative, then it doesn't count toward the contact area. Before each series of images is run, a 'complete contact value' is predetermined by averaging the 90th percentiles of the difference values for a sample of images in the series. If the difference between the gray value and the threshold is higher than this complete contact value, it is counted as one pixel of area. Intermediate differences (between zero and the predetermined complete contact value) are counted by linearly interpolating between zero and one pixel.

Because there were occasionally single dark points in the middle of the tape that appeared from noise in the data, the algorithm makes a third pass to disallow points to be counted as 'in contact' if they had fewer than five neighboring points in the three by three square at which it was centered and fewer than five neighboring points in the four possible three by three squares centered at the corners of that square. This affected very few points.

The parameters above were determined by coloring the contact points red (Fig. 4c) and visually verifying the results. Measured contact areas were checked against careful visual estimates. Parameters and lighting where kept constant throughout testing. The area of each pixel is 0.039mm^2 as calibrated by the ruler in the frame.

C. Measuring the Peeled Area

The peeled area was measured by counting the fuzzy values of the pixels that were in contact in the previous frame but not in contact in the current frame. Only the pixels lower in the frame than the contacting pixels were counted since detachment elsewhere was not peeled by the tension of the foot.

IV. Performance of the Robot

A. Performance of Black Wheel-legs with Flat Profile

When the tape is attached directly to the flat surfaces of the small black wheel-legs (FS Configuration), the performance of the robot is very sensitive to the length of the adhesive. At first, adhesives were cut as long as possible without interfering with other spokes (23mm), but the robot would sometimes detach from the substrate. Although the feet appeared to attach from the view of the approach camera, footage from the contact camera made it clear that no contact area had been formed. However, when the adhesives were trimmed progressively shorter, the robot adhered to the surface better, even though the tape was older, until the tapes were down to 8mm long. At 8mm long, one foot would detach before the next foot had a chance to attach. All subsequent tests were performed with 15mm long feet, which were not observed to buckle during normal locomotion (Figure 5).

At this length, the adhesive contacts the substrate toe-first at six degrees to the substrate. The distal end of the tape attaches to the substrate so lightly that there is no visible contact area. As the tape flattens against the glass, the unattached length gets shorter and stiffer, so the first real contact area is at the proximal end of the tape, near where the tape overhangs from the Delrin® wheel-leg. A relatively small triangular contact area is formed as the previous foot on the same wheel-leg detaches. As the spoke of the wheel-leg rotates past perpendicular to the substrate, more contact is sometimes formed. Then, the tape peels with a line of

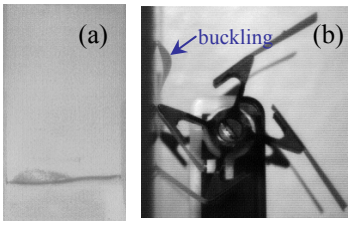

Fig. 5. The maximum contact area (a) of a FS test in which the tape was too long (23mm). Compare to second column of Fig 5a. Occasionally, with longer feet, no contact would form, possibly due to buckling (b).

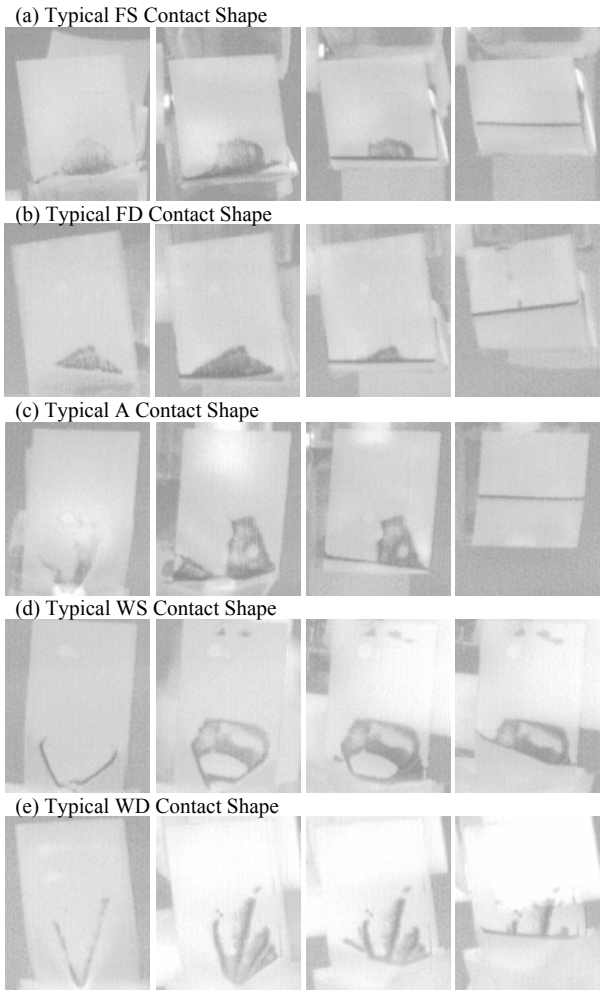

Fig. 6. Images from sample contact videos. The first image is 20 msec after the foot touches the substrate. The second image is the frame in which the largest contact was measured. The third image is from the instant in which the next foot (on the same wheel-leg) touches the substrate, and the last image is from midway between the contact of the next foot and the detachment of this foot. (The one exception is that the second image of part (d) WS is not at max contact area but midway between the first and third images because the max contact occurred just after the contact of the next foot. (See accompanying video)

contact (Fig. 6a). During peeling, the angle between the tape and the substrate (peel angle) starts at about 40 degrees and ends at about 50 degrees. Doubling the tape (FD Configuration) tends to increase the amount of contact area and makes the shape of the area more consistent and compact (Fig. 6b). The peel angle is 40 to 50 degrees.

B. Performance of Black Wheel-legs with Arced Profile

When the same wheel-legs have small rolls of paper attached under a single layer of tape (A Configuration), the tape is arced (Fig. 3b), which makes the climbing more reliable than when there is a single non-arced piece of tape (FS). The tape touches the surface toe-first at an included angle of four degrees to the substrate. The contact area is first formed near the middle, laterally. Because of the increased beam stiffness of the tape, more pressure can be applied to more distal portions of the tape, which is why the contact area is longer, occasionally stretching to nearly 75% of the overhanging tape. Then the contact area spreads out on two sides such that there are two areas, one on the left and the other on the right side of the tape (Fig. 6c).

In this configuration, with very fresh tape, the robot will attach so well that it occasionally stalls on the glass, because more torque is required to peel off the adhesive than the drive motor can provide. After walking about 30 cm, this does not occur and the robot can steadily walk another 250 cm without falling or detaching.

C. Performance of White Wheel-legs

When the larger white wheel-legs with pinned compliant ankles are used, the robot falls from the substrate after 45 cm instead of after 300 cm. Because of the larger spoke length and fewer spokes, greater rolling motions of the robot are seen. Sometimes discrete lurches are observed. As the robot rolls, the load shifts between the left and right feet. Because the torsion spring is weak, the angle of the foot relative to the substrate changes with the load in the foot. During stance, the foot rotates in the sagittal plane, pivoting about the attachment point. The cyclic bending about this point may explain the creases that arise at the proximal end of the overhanging tape, when these wheel-legs are used.

With single tape (WS), the robot forms contact area starting with a shallow ‘V’ shape. The foot comes into contact with the glass toe-first, about 5 to 10 degrees from parallel to the glass. Once contact is made, the torsion spring is loaded and the plastic foot rotates so that it is parallel with the substrate. As the robot rolls back and forth, new areas contact the glass and hold. The contact areas can be very irregular, sometimes stretching all the way up the length of the tape without spanning the width, sometimes forming U-shaped areas. The maximum contact area often occurs after the next foot on the same side touches the substrate. Unlike for the black wheel-legs, a peel-line isn’t visible until after the next foot contacts the substrate (Fig. 6d). Then, it peels at an angle of 55 to 60 degrees. The next foot may interfere with peeling, holding the tape to the glass.

When a double layer of tape is used (WD), the contact area starts out as a smaller sharper V (Fig. 6e). The tape doesn’t flatten out against the substrate and instead the torsion spring is loaded. The tape creases less frequently and the robot runs reliably for more steps.

V. Results of Video Analysis

A. Center Height

The distance between the geometric center of the robot and the substrate, or ‘center height’, was measured from the approach video. This variable is important because it is proportional to the tensile normal forces (adhesion) required to prevent the robot from falling. There was no measurable difference between configurations of the same wheel-legs. The minimum and maximum center height was measured for several trials. The black wheel-legs had average minimum center height of 1.47 cm and average maximum center height of 1.55 cm (n=6). The white wheel-legs had average minimum center height of 1.79 cm and average maximum center height of 2.00 cm (n=7). The averages are

proportional to the rigid leg length (see Table 1). The typical amplitude of oscillation for the white wheel-legs is more than twice that of the black.

B. Timing of Steps and Releases

The robot walked at different speeds in different tests because of the different torque requirements of the different configurations. The value that best represents the pace of the robot is the time between when two sequential feet on the same wheel-leg touch the glass. This pace time was averaged and used to normalize the overlap in time in which two feet of the same wheel-leg were attached to the substrate. The pace times were 0.88 seconds for FS, 0.74 for FD, 0.77 for A, 1.13 for WS, 1.28 for WD. The overlap

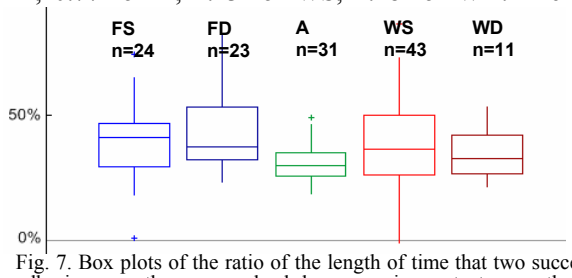

Fig. 7. Box plots of the ratio of the length of time that two successive adhesives on the same wheel leg were in contact over the time between initial contacts of successive feet.

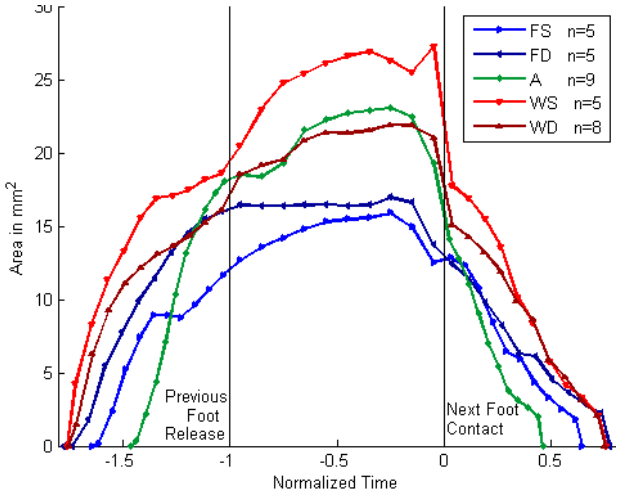

Fig. 8. Averaged contact area vs. time for several runs of each configuration plotted with different timescales such that the release of the previous foot and the contact of the next foot are coincident.

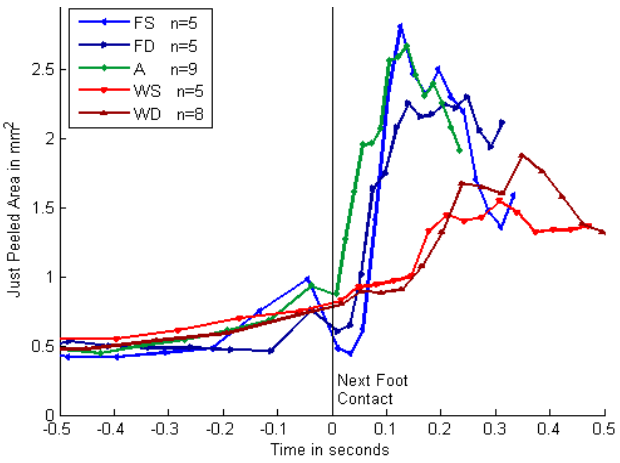

Fig. 9. Area peeled off at each time-step.

values, (with medians of 41.4% for FS, 37.5% for FD, 30.2% for A, 36.3% for WS, and 33.3% for WD) are plotted in Fig. 7. This means that the median percent of the time that only one foot on a side is in contact are 17.2% for FS, 25.0% for FD, 39% for A, 27.4% for WS, and 33.4% for WD.

C. Area Measurements

The measured contact area was different for each step of the same configuration. To determine typical data, each curve in Fig. 8 was divided into three parts based on events observed by the approach camera. The first part of the curve, when the contact area was generally increasing, was between when the foot of interest contacted the substrate and when the previous foot (on the same wheel-leg) detached. The second portion of the data was between the release of the previous foot and the initial contact of the next foot on the wheel-leg. In the second part, the contact area changed more slowly or not at all. The third part of the data was from the time that the next foot on the same wheel-leg contacted the substrate to when the foot of interest detached. The shape of this portion of the curve was different in every test but it usually included a sharp decline in area followed by a low flat line continuing to the end. Each portion of the data was divided into 10 evenly spaced bins and the average value of the curve was found for each bin. To obtain a typical area plot from the individual plots, the bin values from each trial were averaged and plotted in Fig. 8, with a timescale such that the release of the previous foot is at -1 and the start of the application of the next foot is at 0.

The average values of the contact area are generally larger for the white wheel-legs and smaller for the black ones (Fig. 8). For the black wheel-legs, changing the shape of the tape to arced increases the area by as much as a half during the period where only one foot on that wheel-leg is attached. However, the contact areas for all three black wheel-leg configurations are nearly the same size during peeling. On the black wheel-legs, the contact area generally increases with contact stiffness. While on the white-wheel-legs the contact area generally decreases with contact stiffness.

D. Peeled Area Measurements

The peeled areas were averaged similarly and plotted in Fig. 9. The instant in each data set where the next foot on the same wheel-leg made contact were aligned. The reason that the beginning of the graph is not zero is due to high frequency fluctuations in lighting and occasional shifts in contact area. Note that the peel rate for the black feet is higher, and rises sooner after the contact of the next foot.

VI. Discussion

The longer length of the white wheel-legs must be considered when comparing its performance with the black wheel-legs, as the tensile adhesive force can be estimated by the ratio of the distance of the center of mass to the wheelbase times the weight. The center of mass with the white wheel-legs is approximately 30% further from the substrate (as estimated by geometric center height or by leg

length). In addition, with the white wheel-legs the robot weighs slightly more (101 grams, instead of 87 grams). Therefore the WS and WD trials need 1.5 times the adhesive force as the FS, FD, and A trials to avoid falling. When climbing vertically, the longer legs correspond to a proportional increase in the largest step obstacle on the glass wall the robot can climb onto (almost 60% of the center height for both wheel-legs). However, there is no increase in the largest step obstacle the robot could climb off (14.3mm for both wheel-legs).

One measure of the stability of a climbing design is the amount of time that two feet on the same wheel-leg are in contact with the substrate. At slow speeds, this is a quasi-static system and the robot detaches from the glass when no contact area is formed on one front foot. Having a large overlap time reduces the consequence if a foot detaches early or generates contact slowly. In addition, when both feet are in contact, positive pressure can be applied to the attaching foot while the peeling foot supports the moment of the weight of the robot. Fig. 7 shows that the relative overlap times were similar in magnitude for each configuration. Since the climbing reliability of some configurations was much better than others, the similar overlap times suggest this is not a good metric.

While the number of feet in contact was roughly equivalent, the relative amount of contact was not. The contact area in Fig. 8, divided by the leg length, or by the adhesion required, is higher for the A and FD trials than for the WD trials. Having more area in contact with the substrate does not necessarily increase the required force to peel the foot, but it does increase the amount of energy which must be expended to abruptly detach the foot. Therefore larger contact area will increase reliability during small perturbations in the motion. The black wheel-legs were observed to produce smoother center-height motion with smaller oscillations, which may also contribute to the improved tolerance to variations associated with increasingly dirty tape on real substrates.

To obtain good contact, the adhesive must be stiff enough that it is pressed against the substrate. The three black wheel-leg configuration contact areas in Fig. 8 show that stiffening the tape increases the contact area built during attachment, which may be why the robot can climb longer distances with these wheel-legs than with the white ones. The tests on the white wheel-legs demonstrate that compliance at the ankle, in series with the compliance of the adhesive, may absorb the energy that would otherwise deform the adhesive as it conforms to the substrate. For this reason, the contact area of the stiffer WD feet is less than the contact area of the WS feet. (However, the overall performance of the WS feet was worse than the WD feet because of plastic deformation, or creasing, of the adhesive).

The noticeable differences in these results show how important the design of the attachment appendages is to the performance of a climbing vehicle. In all these tests, the width and type of the adhesive, the chassis of the vehicle, and the substrate were all held constant. The dimensions in two sets of wheel-legs were adjusted to improve climbing. The shorter black wheel-legs without compliant ankles allowed vertical climbing for an order of magnitude more trials, each of about 30 cm in length, even though the distance covered by each step was smaller. These principles will be directly applicable to the design of later climbing robots with dry adhesives.

ACKNOWLEDGMENTS

The authors would like to thank Gregory Wile for compiling the accompanying video and Matt Leitch for his assistance in testing and in creating Figure 3c.

REFERENCES

[1] S. Hirose and K. Kawabe, "Ceiling Walk of Quadruped Wall Climbing Robot NINJA-II," *Proc. Int. Conf. on Walking and Climbing Robots* (CLAWAR '98), Brussels, Belgium, 1998.

[2] T. Yano, T. Suwa, M. Murakami, and T. Yamamoto, "Development of a Semi Self-Contained Wall Climbing Robot with Scanning Type Suction Cups," *Proc. Int. Conf. on Intelligent Robots and Systems* (IROS '97), Grenoble, France, 1997.

[3] L. Guo, K. Rogers, and R. Kirkham, "A Climbing Robot with Continuous Motion," *Proc. Int. Conf. on Robotics and Automation* (ICRA '94), 1994.

[4] R. Lal Tummala, R. Mukherjee, N. Xi, et al., "Climbing The Walls," *IEEE Robotics and Automation Magazine,* vol. 9, no. 4, pp. 10–19, 2002.

[5] L. Illingworth and D. Reinfeld. "Vortex Attractor for Planar and Non-planar Surfaces," U.S. Patent 6,619,922, Sep. 16, 2003.

[6] T. Bretl, S. Rock, J. C. Latombe, B. Kennedy, and H. Aghazarian, "Free-Climbing with a Multi-Use Robot," *Proc. Int. Symp. on Experimental Robotics* (ISER), Singapore, 2004

[7] K. Autumn, M. Buehler, M. Cutkosky, et al. "Robots in Scansorial Environments," *Proc. of SPIE,* Vol. 5804, pp 291–302. 2005.

[8] S.F. Frazier, G.S. Larsen, D. Neff, , et al. "Elasticity and Movements of the Cockroach Tarsus in Walking," *J. Comp. Physiol. A*, vol. 185, pp. 157–172. 1999.

[9] K. Sangbae, A.T. Asbeck, M.R. Cutkosky, and W.R. Provancher "SpinybotII: Climbing Hard Walls with Compliant Microspines," *Int. Conf. on Advanced Robotics*, Seattle, USA. 2005.

[10] K. Autumn, Y.A. Liang, S.T. Hsieh, et al. "Adhesive force of a single gecko foot-hair," *Nature*, vol. 405, pp. 681–685. 2000

[11] A. Peressadko and S.N. Gorb "When Less is More: Experimental Evidence For Tenacity Enhancement by Division of Contact Area," *J. Adhesion*, vol. 80, pp. 1–15. 2001

[12] M. Sitti and R.S. Fearing "Synthetic Gecko Foot-Hair Micro/Nano-Structures for Future Wall-Climbing Robots," *Int. Conf. on Robotics and Automation* (ICRA '03), Taipei, Taiwan. 2003.

[13] C. Menon, M. Murphy, and M. Sitti "Gecko Inspired Surface Climbing Robots," IEEE ROBIO '04, Shenyang, China. 2004.

[14] Robo-Gecko, *Discover*, September 2000.

[15] S. Niederegger and S. Gorb, "Tarsal movements in flies during leg attachment and detachment on a smooth substrate," *J. Insect Physiol*., vol. 49, pp. 611–620, 2003.

[16] J.M. Morrey, B.G.A. Lambrecht, A.D. Horchler, R.E. Ritzmann, and R.D. Quinn "Highly Mobile and Robust Small Quadruped Robots," *Int. Conf. on Intelligent Robots and Systems* (IROS '03), pp. 82–87, Las Vegas, USA, 2003.

[17] A. Martin-Alvarez, W. De Peuter, J. Hillebrand, et al., "Walking Robots for Planetary Exploration Missions," *Proc. 2nd World Automation Congress* (WAC '96), Montpellier, France, 1996.

[18] U. Saranli, M. Buehler, and D. Koditschek, "RHex: A Simple and Highly Mobile Hexapod Robot," *Int. J. Robotics Research,* vol. 20, no. 7, pp. 616–631, 2001.

[19] R.D. Quinn, G.M. Nelson, R.E. Ritzmann, R.J. Bachmann, D.A. Kingsley, J. Offi, and T.J. Allen., "Parallel Strategies for Implementing Biological Principles Into Mobile Robots," *Int. Journal of Robotics Research,* Vol. 22 (3) pp. 169-186. 2003

[20] K.A. Daltorio, A.D. Horchler, S. Gorb, R.E. Ritzmann, and R.D. Quinn "A Small Wall-Walking Robot with Compliant, Adhesive Feet," *Int. Conf. on Intelligent Robots and Systems* (IROS '05), Edmonton, Canada. 2005.

[21] K.A. Daltorio, S. Gorb, A. Peressadko, A.D. Horchler, R.E. Ritzmann, and R.D. Quinn "A Robot that Climbs using Micro-Structured Polymer Feet," *Int. Conf. on Climbing and Walking Robots* (CLAWAR '05), London, England. 2005.

[22] T.E. Wei, K.A. Daltorio, S.N. Gorb, L. Southard, R.E. Ritzmann, and R.D. Quinn "A Small Climbing Robot with Compliant Ankles and Multiple Attachment Mechanisms," *Int. Conf. on Climbing and Walking Robots* (CLAWAR '06), Brussels, Belgium. 2006.